International Journal of Engineering & Technology, 7(4.16) (2018) 37-41

International Journal of Engineering & Technology

Website: www.sciencepubco.com/index.php/IJET

Research paper

2D Finite Element Modeling and Analysis of Dry Turning Process of Aeronautic Aluminium Alloy 2024

Hassan Ijaz[1]*, Waqas Saleem[1], Muhammad Asad[2], Ahmed Alzahrani[1], Tarek Mabrouki[3]

[1]*Mechanical Engineering Department, University of Jeddah, Jeddah, Saudi Arabia*
[2]*Mechanical Engineering Department, Prince Mohammad Bin Fahd University, AlKhobar, Saudi Arabia*
[3]*Mechanical Engineering Department, University of Tunis El Manar, ENIT, Tunis, Tunisia*
**Corresponding author E-mail:hassan605@yahoo.com*

Abstract

The identification and selection of different physical parameters greatly influence the machining of materials. Cutting speed, feed, tool rake angle and friction are important physical parameters that affect the machining of the materials. Selection of suitable cutting parameters can help to achieve the better machining quality and enhanced tool life. Properly defined FE-model can efficiently simulate the machining processes and thus may help to save the machining cost and expensive materials instead of performing real-life experiments. In the present work, a detailed finite element analysis on the orthogonal cutting of aluminium alloy (AA2024) is conducted to validate the FE-based machining model. Numerically obtained resultant cutting forces are successfully compared with the experimental results for 0.3 and 0.4 mm/rev cutting feeds with 17.5° tool rake angle. Subsequently, the cutting forces are predicted for the selected feeds of 0.35 & 0.45 mm/rev and for different tool rake angles like 9.5°, 13.5° & 21.5° using finite element analysis. Finally, the optimum cutting parameters are suggested for cutting AA2024.

Keywords: *Finite element analysis; AA2024; Johnson-Cook Material model; Damage evolution; Turning process.*

1. Introduction

The aeronautical grade aluminium alloy 2024 (AA2024) is widely used in various engineering applications because of its excellent mechanical properties. This particular material goes under various machining processes before taking the designed shape of the finished product and thus experience severe cutting forces [1-2]. The different cutting parameters like cutting speed, feed, tool rake angle, and workpiece/tool interface friction affect the machining quality and chip formation morphology [3]. An exhaustive experimentation is required to determine the optimum cutting parameters that can enhance the machining quality and effective tool life. The finite element analysis can provide the alternate solution to the expensive experimentation provided that required material properties are available [4-5]. Different researchers performed finite element analysis to simulate the machining processes of metallic materials [6-11].

The cutting procedure in metals may be simulated using two established approaches i.e. fracture mechanics and damage mechanics. Fracture mechanics assumes that a crack is already present in the component and energy is required to propagate it further [12]. Damage mechanics not only deals with the propagation of a crack but can also deal with the initiation of a crack [13-14]. The later approach is adopted in the current study to simulate the machining process. A damage layer of the order of tool tip radius is modelled between workpiece support and chip. This damaged layer is modelled with Johnson-Cook plasticity material behaviour coupled with damage evolution law. Various researchers used Johnson-Cook plasticity coupled damage model to successfully simulate the machining process in metals [15-17].

In this article, a comprehensive 2D finite element analysis study is carried out to simulate the orthogonal cutting process of AA2024. Commercially available finite element software ABAQUS/Explicit is used to model and simulate the machining process. Finite element (FE) simulations are performed considering different cutting parameters like cutting speed, feed, tool rake angle and friction effect at the workpiece/tool interface surfaces. Numerically acquired cutting forces results are compared with the experimental results for 0.3 and 0.4 mm/rev feeds with 17.5° rake angle [4]. In addition, two more feeds (0.35 and 0.45 mm/rev) and three different rake angles (9.5°, 13.5° and 21.5°) are selected for FE simulations and resultant cutting forces are predicted for the orthogonal cutting process of AA2024.

This article is organized as follows: the selected Johnson-Cook plasticity coupled damaged material model is explained in section 2. Finite element modeling and analysis considering various cutting parameters is described in section 3 and finally concluding remarks are presented in section 4.

2. Material Model for FE-Analysis

Plasticity and damaged coupled Johnson-Cook (JC) material model will be employed for the FE simulations of cutting and chip formation processes [18]. JC model describes the material behaviour taking into account the high strain rates, large strains and temperature dependant viscoplasticity effects [18-19]. Consider that $\bar{\sigma}$ is the plastic flow stress then following relation can be expressed [18]:

$$\bar{\sigma} = \underbrace{\left(\sigma_y + B\bar{\varepsilon}^{n}\right)}_{\text{Plastic term}} \underbrace{\left[1 + C\ln\left(\frac{\dot{\bar{\varepsilon}}}{\dot{\bar{\varepsilon}}_0}\right)\right]}_{\text{Viscosity term}} \underbrace{\left[1 - \left(\frac{T - T_{\text{room}}}{T_{\text{melt}} - T_{\text{room}}}\right)^{m}\right]}_{\text{Softening term}} \quad (1)$$

Where; A, B and n are the strain hardening material constants; C is strain hardening rate constant, m is thermal softening material constant, T_{room} represents the reference ambient temperature and T_{melt} is the melting temperature of the considered material. $\bar{\varepsilon}$ is the equivalent plastic strain, $\dot{\bar{\varepsilon}}$ and $\dot{\bar{\varepsilon}}_0$ are the plastic strain rate and reference strain rate respectively. σ_y is material's yield strength. If one assumes that $\dot{\bar{\varepsilon}}_{0i}$ is the plastic strain at damage initiation then expressed by the following relation [19]:

$$\bar{\varepsilon}_{0i} = \left[D_1 + D_2 \exp\left(D_3 \frac{P}{\bar{\sigma}}\right)\right]\left[1 + D_4 \ln\left(\frac{\dot{\bar{\varepsilon}}}{\dot{\bar{\varepsilon}}_0}\right)\right]\left[1 + D_5\left(\frac{T - T_{\text{room}}}{T_{\text{melt}} - T_{\text{room}}}\right)\right] \quad (2)$$

In the above equation, P is the pressure stress and $D_1 \sim D_5$ are the experimentally determined damage constants. Different JC parameters for AA2024 are given in Table 1. During the FE computations, the damage is initiated when a scalar parameter ω exceeds 1 and is expressed as follows [20]:

$$\omega = \frac{\sum \Delta\bar{\varepsilon}}{\bar{\varepsilon}_{0i}} \quad (3)$$

Following energy-based criteria is adopted for the initiation and propagation of fracture in the material [4] [13]:

$$G_f = \int_0^{\bar{u}_f} \sigma_y d\bar{u} \quad (4)$$

Where; G_f and $\bar{u}_f$ are energy and equivalent plastic displacement at fracture respectively. This equivalent plastic displacement can be expressed using the following relation [21]:

$$\bar{u}_f = \frac{2G_f}{\sigma_Y} \quad (5)$$

Fracture energy required for mode I and II crack growth can be calculated using the relation given below [4]:

$$\left(G_f\right)_{I,II} = \left(\frac{1-\upsilon^2}{E}\right)\left(K_C^2\right)_{I,II} \quad (6)$$

Here, K_{IC} and K_{IIC} are the mode I and II fracture toughness and their values are $K_{IC} = 26$ (MPa $\sqrt{m}$) and $K_{IIC} = 37$ (MPa $\sqrt{m}$) [4]. E is the modulus of elasticity of the material and υ is the Poisson ratio. If D is defined as scalar damage variable then it can be represented by linear or exponential damage evolution laws [4].

$$D = \frac{\bar{u}}{\bar{u}_f} \text{ (Linear)}; \; D = 1 - \exp\left(-\int_0^{\bar{u}} \frac{\bar{\sigma}}{G_f} d\bar{u}\right) \text{ (Exponential)} \quad (7)$$

The uni-axial stress-strain response for linear and exponential damage evolution laws is shown in Fig. 1 and properties of different JC parameters are listed in Table 1.

3. Finite Element Analysis

In this section, 2D FE analysis results are presented and discussed for the orthogonal cutting process of AA2024 with different cutting parameters such as cutting speed (V), tool rake angle (γo), feed (f) and friction coefficient (μ). All the simulations are performed in ABAQUS/Explicit using coupled temperature-displacement four node quadrilateral continuum elements with plane strain assumption (CPE4RT).

The workpiece and tool geometries along with necessary boundary conditions are shown in Fig. 2. The workpiece is divided into three parts as: 1) chip 2) damage zone 3) workpiece support. The size of the damage zone is of the order of the tool tip radius [22]. A Coulomb friction model is used between the tool and workpiece surfaces [4]. Moreover, chip also makes self contact. During the FE analysis the tool will interact and follow the damage zone path. The properties of the workpiece and tool are given in Table I. FE analysis results of cutting forces are compared with the experimental results for orthogonal cutting of AA2024 [4].

Table 1: Workpiece and Tool Properties for AA2024 [4]

Physical parameter	Work piece (AA2024)	Tool
Density, ρ (Kg/m^3) at 25°C	2700	11900
Poisson ratio, v	0.33	0.22
Specific heat C_p (T) (JKg^{-1}°C^{-1})	C_p = 0.557 T + 877.6	400
Thermal conductivity λ (T) (Wm^{-1}C^{-1})	25≤T≤300: λ = 0.247T+114.4 300≤T≤T_{melt}: λ = -0.125T+226.0	50
Expansion, α (mm^{-1}°C^{-1})	α + 8.9 x 10^{-3} T + 22.2	-
T_{melt}, (°C)	520	-
T_{room} (°C)	25	25
JC Parameters		
σ_y = 352 *MPa*; *B* = 440 *MPa*; *n* = 0.42; *C* = 0.0083; *m* = 1; *D1* = 0.13 *D2* = 0.13; *D3* = -1.5; *D4* = 0.011; *D5* = 0		

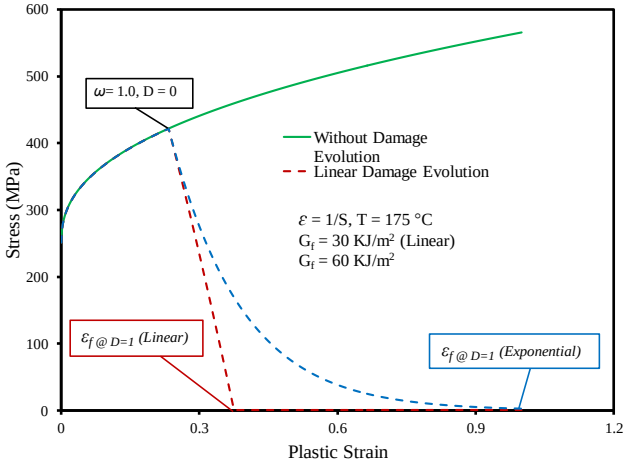

Fig. 1: Stress-strain behaviour for JC material model

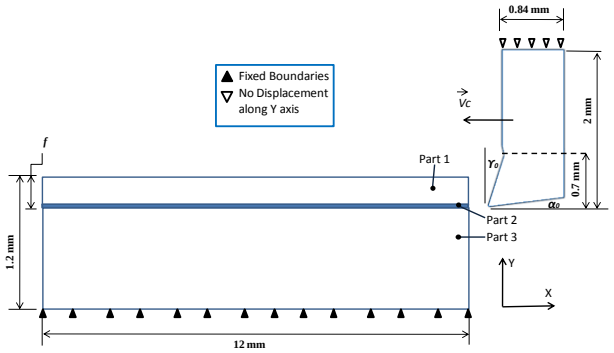

Fig. 2: Workpiece and Tool geometries. V_c = Cutting Velocity, γ_0 =Rake angle, α_0 = Clearance angle, f = Chip Thickness.

The reaction cutting force obtained from FE analysis for cutting speed of 800 m/min, a feed of 0.4 mm/rev and rake angle of 17.5° for two different friction coefficients (0.15 and 0.1) is shown in Fig. 3. The FE results are compared with the experimental one and experimental results for 0.3 and 0.4 mm/rev feeds for different cutting speeds. Both figures show acceptable errors when FE results are compared with experimental. Though maximum error obtained for a small feed of 0.3 mm/rev is slightly high (9.1%) in comparison of larger feed of 0.4 mm/rev (6.1%) for cutting speed of 200 m/min.

Fig. 7 shows the variation of cutting force by varying the feed and friction coefficients. The maximum variation is 5.7 % and minimum variation is 3 % by changing the friction coefficient value from 0.15 to 0.1. Moreover, this variation in cutting force decreases as the cutting speed increases.

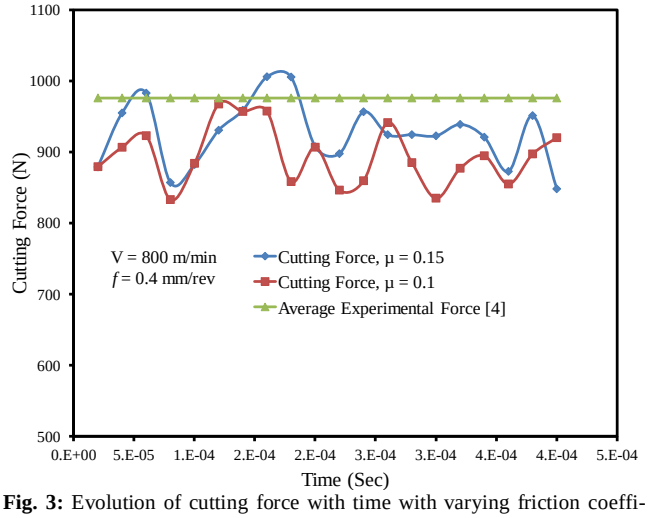

Fig. 3: Evolution of cutting force with time with varying friction coefficients

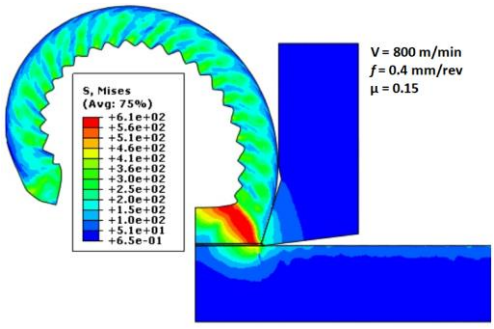

Fig. 4: Mises stress profile on chip formation (Cutting speed of 800 m/min and feed of 0.4 mm/rev)

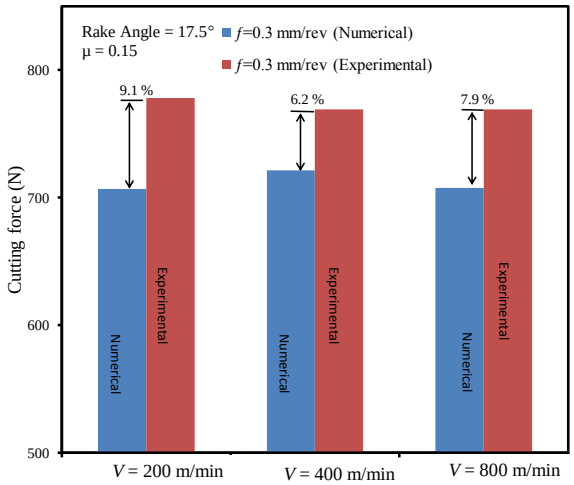

Fig. 5: FE analysis vs Experimental results [4] for 0.3 mm/rev feed

are found to be in good agreement. One can also observe that friction coefficient with a value of 0.15 produced relatively much better results. Fig. 4 shows the Mises stress distribution. Fig.5 and Fig. 6 show the comparison of FE obtained results with the

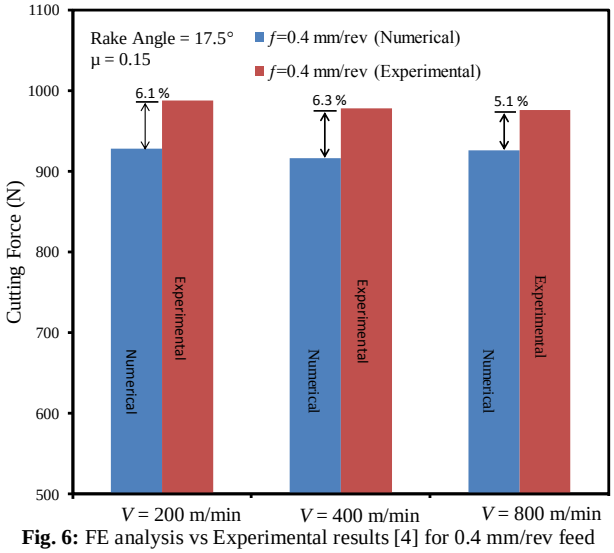

Fig. 6: FE analysis vs Experimental results [4] for 0.4 mm/rev feed

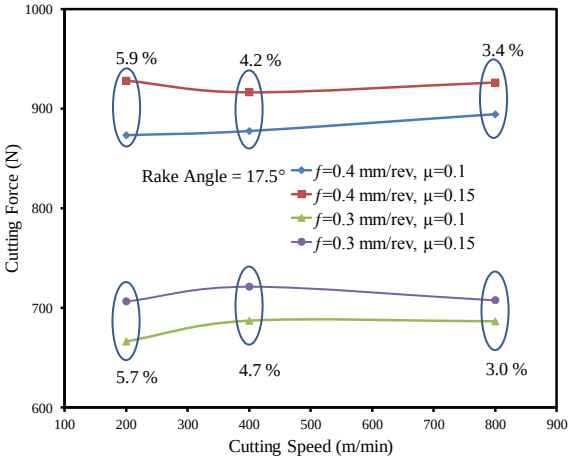

Fig. 7: Cutting force vs Cutting speed with varying feeds and friction coefficients

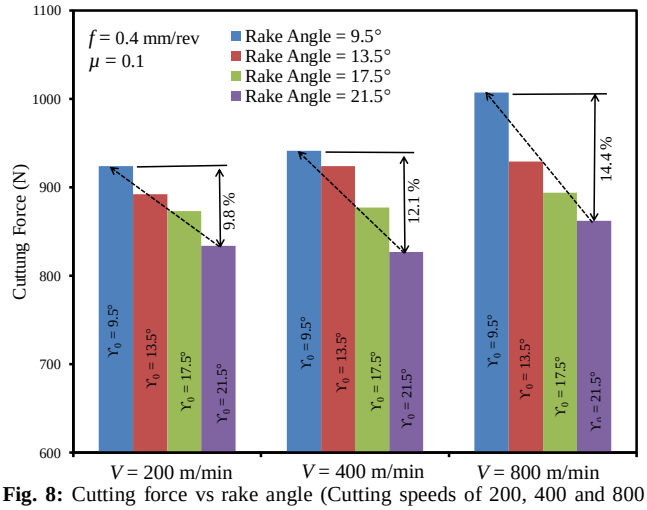

Fig. 8: Cutting force vs rake angle (Cutting speeds of 200, 400 and 800 m/min)

Fig. 8 presents the variation of cutting force by varying the tool rake angle for three different cutting speeds. One can observe that the cutting force increases as the tool rake angle decreases i.e. cutting force changes by 9.8% by changing the rake angle for

cutting speed of 200 m/min. It is evident that the variation in the cutting force increases with the increase in cutting speed i.e. it increases from 9.8% to 14.4% as the cutting speed changes from 200 to 800 m/min.

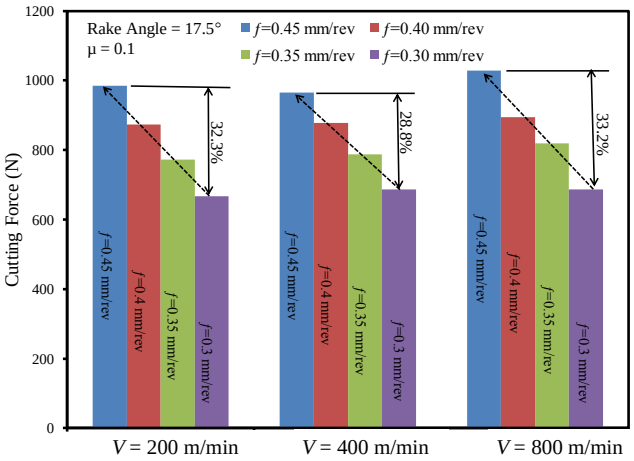

Fig. 9: Cutting force vs Feed (Cutting speeds of 200, 400 and 800 m/min) with varying feeds

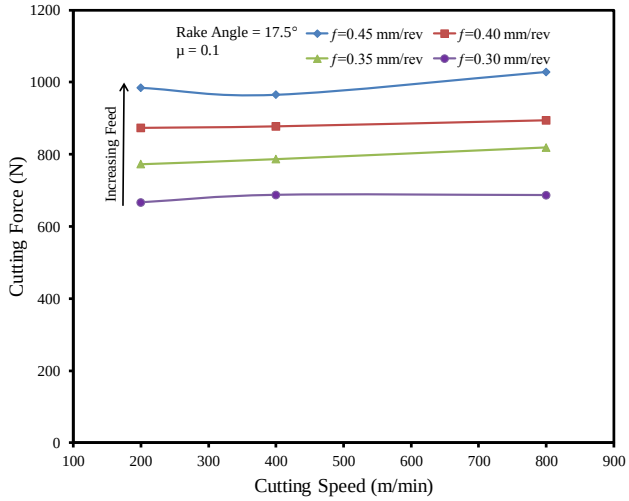

Fig. 10: Cutting force vs Cutting speed

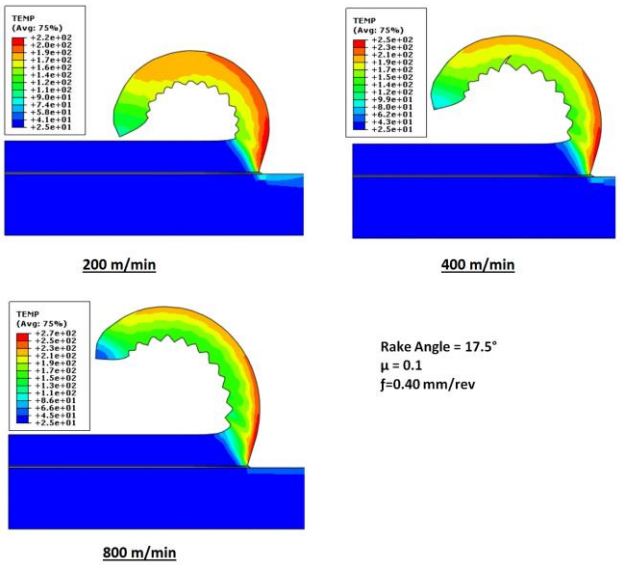

Fig. 11: Temperature profile with varying cutting speeds

Fig. 9 present the variation of cutting force with cutting speed for various cutting feeds. It cab seen that cutting force rises almost linearly (32.3%) as the feed is increased from 0.3 to 0.45 mm/rev for 200 m/min cutting speed. An observation can also be made from Fig. 10 that cutting force does not increase appreciably as the cutting speed increases from 200 t0 800 m/min if other parameters like feed, friction coefficient, and rake angle are kept constant. This particular observation can also be made from Fig. 7. Fig. 11 depicts the temperature profiles during the chip formation simulations for varying cutting speeds. Maximum temperature increases from 220 °C to 270 °C as the cutting speed increases from 200 to 800 m/min.

4. Conclusion

In this article finite element modeling and analysis is performed for different cutting parameters like cutting speed, feed, friction coefficient and tool rake angle. The effect of different varying cutting parameters is studied in detail for the orthogonal cutting of AA2024. The authenticity of FE analysis results is confirmed by comparing it with experimental results for 0.3 & 0.4 mm/rev feed and 200, 400 & 800 m/min cutting speeds for the tool rake angle of 17.5°. Then FE simulations are performed to predict the results for 0.35 & 0.45 m/min feeds by varying tool rake angles (9.5°, 13.5° & 21.5°) for different cutting speeds. It is observed from the FE results that cutting force varies maximum by 9.8% and 14.4% for cutting speeds of 200 and 800 m/min respectively if tool rake angles are changed from 9.5° to 21.5°. It is noted that cutting force varies around 32%-33% approximately for cutting speeds of 200 and 800 m/min if the feed is changed from 0.3 to 0.45 mm/rev. Finally, a temperature range of 220 °C to 270 °C is predicted by changing cutting speeds from 200 to 800 m/min. Later, can help to select suitable cutting tool materials.

References

[1] Nicolaou P, Thurston DL & Carnahan JV, "Machining quality and cost estimation and tradeoffs," Journal of Manufacturing Science and Engineering, Vol. 124, (2002), pp. 840-851.

[2] Sreejith PS & Ngoi BKA, "Dry machining: machining of the future," Journal of Materials Processing Technology, Vol. 101, (2000), pp. 287-291.

[3] Ijaz H, Zain-ul-abdein M, Saleem W, Asad M & Mabrouki T, "A numerical approach on parametric sensitivity analysis for an aeronautic aluminium alloy turning process," Mechanics, Vol. 22, (2016), PP. 149-155.

[4] Asad M, "Elaboration of concepts and methodologies to study peripheral down-cut milling process from macro-to-micro scales," PhD Dissertation, INSALyon, Lyon, France, 2010.

[5] Asad M, Ijaz H, Khan MA, Mabrouki T & Saleem W, "Turning modeling and simulation of an aerospace grade aluminum alloy using two-dimensional and three-dimensional finite element method," Proceedings of the Institution of Mechanical Engineers, Part B: Journal of Engineering Manufacture, Vol. 228, (2014), pp. 367-375.

[6] Agmell M, Ahadi A & Stahl J–E, "Identification of plasticity constants from orthogonal cutting and inverse analysis," Mechanics of Materials, Vol. 77, (2014), pp. 43-51.

[7] Yin CJ, Zheng QC & Hu YH, "Finite element simulation of Titanium alloy turning process," Applied Mechanics and Materials, Vol. 391, (2013), pp. 14-17.

[8] Wu H & Guo L, "Machinability of Titanium alloy TC21 under orthogonal turning process," Materials and Manufacturing Processes, Vol. 29, (2014), pp. 1441- 1445.

[9] Ijaz H, Zain-ul-abdein M, Saleem W, Asad M & Mabrouki T, "Modified Johnson-Cook Plasticity Model with Damage Evolution: Application to Turning Simulation of 2XXX Aluminium Alloy," Journal of Mechanics, Vol. 33, (2017), pp.777-788.

[10] Ijaz H, Zain-ul-abdein M, Saleem W, Asad M & Mabrouki T, "Numerical simulation of the effects of elastic anisotropy and grain size upon the machining of AA2024," Machining Science and Technology, Vol. 22, (2018), pp.522-542.

[11] Liu K & Melkote SN, "Finite element analysis of the influence of tool edge radius on size effect in orthogonal micro-cutting process," International Journal of Mechanical Sciences, Vol. 49, (2007), pp. 650-660.

[12] Meng Q & Wang Z, "Extended finite element method for power-law creep crack growth," Engineering Fracture Mechanics, Vol. 127, (2014), pp. 148-160.
[13] Gornet L & Ijaz H, "High cycle fatigue damage model for delamination crack growth in CF/Epoxy composite laminates," International journal of Damage Mechanics, Vol. 20, (2011), pp. 783-807.
[14] Ijaz H, Saleem W, Zain-ul-abdein Z, Taimoor AA & Mahfouz ASB, "Fatigue delamination crack growth in GFRP composite laminates: mathematical modelling and FE simulation," International Journal of Aerospace Engineering, Vol. 2018, (2018), Article ID 2081785, 8 pages.
[15] Mabrouki T, Girardin F, Asad M & Rigal J-F, "Numerical and experimental study of dry cutting for an aeronautic aluminium alloy (A2024-T351)," International Journal of Machine Tools & Manufacture,Vol. 48, (2008), pp. 1187-1197.
[16] Zhang Y, Outeiro JC & Mabrouki T, "On the selection of Johnson-Cook constitutive model parameters for Ti-6Al-4 V using three types of numerical models of orthogonal cutting," Procedia CIRP, Vol. 31, (2015), pp. 112-117.
[17] Shrot A & Baker M, "Determination of Johnson-Cook parameters from machining simulations," Computational Materials Science, Vol. 52, (2012), pp. 298-304.
[18] Johnson GR & Cook WH, "A constitutive model and data for metals subjected to large strains, high strain rates and high temperatures," Proceedings of the 7th International Symposium on Ballistics, The Hague, Vol. 21, (1983), pp. 541–547.
[19] Johnson GR & Cook WH. Cook, "Fracture characteristics of three metals subjected to various strains, strain rates, temperatures and pressures," Engineering Fracture Mechanics, Vol. 2, (1985), pp. 31–48.
[20] Han ZY, Huang XG, Cao YG & Xu JQ, "A non linear cumulative evolution model for corrosion fatigue damage," Journal of Zhejiang University Science A, Vol. 15, (2014), pp. 447-453.
[21] Shi J. & Liu CR, "On predicting chip morphology and phase transformation in hard machining," The International Journal of Advanced Manufacturing Technology, Vol. 27, (2006), pp. 645-654.
[22] Subbiah S & Melkote SN, "Effect of finite edge radius on ductile fracture ahead of the cutting tool edge in micro-cutting of Al2024-T3," Materials Science and Engineering: A, Vol. 474, (2008), pp. 283-300.